Journal of Experimental Botany, Vol. 63, No. 1, pp. 489–502, 2012
doi:10.1093/jxb/err294 Advance Access publication 6 October, 2011
This paper is available online free of all access charges (see http://jxb.oxfordjournals.org/open_access.html for further details)

Journal of Experimental Botany
www.jxb.oxfordjournals.org

RESEARCH PAPER

Leaf optical properties reflect variation in photosynthetic metabolism and its sensitivity to temperature

Shawn P. Serbin*, Dylan N. Dillaway†, Eric L. Kruger and Philip A. Townsend

Department of Forest and Wildlife Ecology, University of Wisconsin-Madison, 226 Russell Labs, 1630 Linden Drive, Madison, WI 53706, USA

† Present address: School of Forestry, Louisiana Tech University, Ruston, LA 71270, USA
* To whom correspondence should be addressed. E-mail: serbin@wisc.edu

Received 12 May 2011; Revised 15 August 2011; Accepted 22 August 2011

Abstract

Researchers from a number of disciplines have long sought the ability to estimate the functional attributes of plant canopies, such as photosynthetic capacity, using remotely sensed data. To date, however, this goal has not been fully realized. In this study, fresh-leaf reflectance spectroscopy (λ=450–2500 nm) and a partial least-squares regression (PLSR) analysis were used to estimate key determinants of photosynthetic capacity—namely the maximum rates of RuBP carboxylation (V_{cmax}) and regeneration (J_{max})—measured with standard gas exchange techniques on leaves of trembling aspen and eastern cottonwood trees. The trees were grown across an array of glasshouse temperature regimes. The PLSR models yielded accurate and precise estimates of V_{cmax} and J_{max} within and across species and glasshouse temperatures. These predictions were developed using unique contributions from different spectral regions. Most of the wavelengths selected were correlated with known absorption features related to leaf water content, nitrogen concentration, internal structure, and/or photosynthetic enzymes. In a field application of our PLSR models, spectral reflectance data effectively captured the short-term temperature sensitivities of V_{cmax} and J_{max} in aspen foliage. These findings highlight a promising strategy for developing remote sensing methods to characterize dynamic, environmentally sensitive aspects of canopy photosynthetic metabolism at broad scales.

Key words: J_{max}, leaf mass per unit area, leaf optical properties, leaf reflectance, nitrogen, photosynthesis, temperature, V_{cmax}.

Introduction

Using an array of technologies, researchers from a number of disciplines continue to pursue methods for remotely estimating the biochemical, structural, and physiological traits of plant leaves and canopies based on their optical properties (Wessman *et al.*, 1988*b*; Martin and Aber, 1997; Smith *et al.*, 2002; Biewer *et al.*, 2009). Thus far, target foliar traits have included concentrations of nitrogen (N_{mass}, Bolster *et al.*, 1996; Gillon *et al.*, 1999), lignin, cellulose (Wessman *et al.*, 1988*a*; Martin and Aber, 1997; Kokaly and Clark, 1999; Petisco *et al.*, 2006), and photosynthetic pigments (Richardson *et al.*, 2002; Gitelson *et al.*, 2003; Moorthy *et al.*, 2008) as well as water content (Sims and Gamon, 2003; Stimson *et al.*, 2005; Cheng *et al.*, 2008). In addition, leaf isotopic ratios ($\delta^{13}C$ and $\delta\ ^{15}N$; Richardson and Reeves, 2005; Wang *et al.*, 2007; Kleinebecker *et al.*, 2009), specific leaf area (SLA; Asner and Martin, 2008), and leaf mass per area (LMA; Asner *et al.*, 2011; Doughty *et al.*, 2011) have been successfully estimated using leaf optical properties. To date, however, remote sensing of leaf functional attributes, such as photosynthetic metabolism, has not progressed as rapidly (Grace *et al.*, 2007).

Much of the effort to relate optical remote sensing data to photosynthetic status and ecosystem function has focused on the use of the photochemical reflectance index (PRI, Gamon *et al.*, 1992, 1997). The PRI, which provides a linkage with photosystem II (PSII) efficiency by tracking the variation in xanthophyll cycle pigments, has been successfully used to assess photosynthetic functioning

across a range of vegetation types (Peñuelas *et al.*, 1995, 1998; Gamon *et al.*, 1997; Nichol *et al.*, 2000; Stylinski *et al.*, 2000; Guo and Trotter, 2004; Fuentes *et al.*, 2006; Drolet *et al.*, 2008; Hilker *et al.*, 2008; Middleton *et al.*, 2009) and responses of plants to environmental stress (Dobrowski *et al.*, 2005; Suarez *et al.*, 2008; Gray *et al.*, 2010).

A parallel avenue of research has focused on the detection of vegetation chlorophyll fluorescence (CF) to exploit its relationship with photosynthetic functioning (Freedman *et al.*, 2002; Louis *et al.*, 2005; van der Tol *et al.*, 2009; Damm *et al.*, 2010). CF has been detected through passive monitoring of solar-induced steady-state fluorescence (Zarco-Tejada *et al.*, 2003; Dobrowski *et al.*, 2005; Grace *et al.*, 2007; Campbell *et al.*, 2008) and active laser-induced methods (Ananyev *et al.*, 2005). Although remote sensing of CF remains experimental owing to a variety of technical issues (Grace *et al.*, 2007; Coops *et al.*, 2010), the recent creation of regional and global CF maps using space-borne observations (Guanter *et al.*, 2007; Joiner *et al.*, 2011) highlights the technique's potential.

The results of an effort to further explore the links between the photosynthetic and optical properties of tree leaves are summarized here. Specifically, in a glasshouse study of trembling aspen (*Populus tremuloides*) and eastern cottonwood (*Populus deltoides*) trees grown under different temperature regimes, it was assessed whether climate-mediated variation in leaf photosynthetic metabolism could be effectively estimated using data from visible and near-infrared reflectance spectroscopy (VIS/NIRS). With respect to photosynthetic metabolism, the focus was on two important parameters, the maximum rate at which ribulose *bis*phosphate (RuBP) is carboxylated (V_{cmax}) and regenerated (J_{max}). With robust estimates of these two traits, the photosynthetic performance of a given leaf can be predicted using a widely adopted biochemical model (Farquhar *et al.*, 1980; Farquhar and von Caemmerer, 1982). This model has been effectively scaled to the canopy level (Medlyn *et al.*, 2005; Thum *et al.*, 2007), and its use in canopy and ecosystem process models is increasingly common.

V_{cmax} and J_{max} vary substantially across plant species, functional groups, and growth environments (Wullschleger, 1993; Kattge *et al.*, 2009). Moreover, both parameters are very sensitive to short-term (i.e. seconds to hours) dynamics in leaf temperature (Medlyn *et al.*, 2002; Kattge and Knorr, 2007). The accuracy and credibility of outputs from process models would increase considerably if a feasible methodology were developed for remotely sensing canopy photosynthetic capacity and its temperature sensitivity across broad scales.

The principal objectives of our study were (i) to develop spectroscopic models for estimating V_{cmax} and J_{max} based on leaf data collected across a wide range of growth temperature regimes; and (ii) to assess the effectiveness of those models in estimating the short-term temperature sensitivity of V_{cmax} and J_{max} in the field. The second objective was addressed with measurements of leaf traits in field-grown aspen trees.

Materials and methods

Glasshouse treatments and experimental design

The relationships were tested between leaf photosynthetic and optical properties in climate-controlled glasshouses at the University of Wisconsin–Madison Biotron. Aspen and cottonwood germinants were reared in flats until they reached a height of about 20 cm. Seedlings were then transplanted into 4-litre pots and transferred to the Biotron glasshouses, where they were grown for 8 weeks under one of three different temperature regimes, with fixed day/night air temperatures of 30/23, 25/18, and 20/13 °C. These thermal regimes were chosen to span ranges in air temperature observed during the growing season along a latitudinal transect for a study that examined the physiological factors limiting geographic distributions of temperate and boreal tree species (Dillaway and Kruger, 2010). Each regime was replicated in two glasshouses.

Measurements of leaf gas exchange

During the fourth and eighth weeks of growth in the Biotron glasshouses, leaf gas exchange was measured on a total of 8–10 trees per species in each treatment (4–5 per species and glasshouse, n=78) using a LI-6400 portable photosynthesis system (Li-Cor Biosciences, Lincoln, NE, USA). All measurements were conducted on the youngest, fully expanded leaf of each tree. Leaves were measured under high light intensities (photosynthetic photon flux=1800 μmol m^{-2} s^{-1}, provided by a red-blue LED array) at several CO_2 partial pressures (pCO_2) ranging from 7.5 to 120 Pa. Photosynthesis (A) was assessed first at a cuvette reference pCO_2 of 40 Pa, and then again after each of three step-wise decreases in pCO_2 (i.e. at 25, 15, and 7.5 Pa). Photosynthesis was then measured at 60, 90, and 120 Pa CO_2, respectively. Cuvette reference pCO_2 was controlled using the LI-6400 CO_2 injector system. The potentially confounding influences of diffusion leaks across the cuvette gasket on gas exchange calculations were taken into account by applying the manufacturer's equation to determine the gasket diffusion coefficient (Anonymous, 2005).

At a given pCO_2, leaves were allowed to acclimate to cuvette conditions for 2–5 min, depending on when photosynthetic rate stabilized. Vapour pressure deficit between leaf and air in the cuvette ranged from 0.95–2.01 kPa. For each leaf, the photosynthetic response to pCO_2 was assessed at the daytime air temperature of each treatment (20, 25, and 30 °C), which, owing to concerns about IRGA signal stability, was maintained through the manipulation of cuvette rather than leaf temperature. Thus, because leaf temperature was not directly controlled, it ranged from 20.40–21.80, 25.06–26.14, and 30.05–30.40 °C at the target temperatures of 20, 25, and 30 °C, respectively. Measurements were conducted throughout the day, as long as stomatal conductance remained comparatively high (within 25% of the daily maximum).

Measurement of leaf optical properties

Reflectance was measured for both species on the same leaves assessed for gas exchange using a high-spectral-resolution ASD FieldSpec® 3 Full-Range (350–2500 nm) spectroradiometer (Analytical Spectral Devices, Boulder, CO, USA). All measurements occurred on the leaf adaxial surface using a leaf-clip assembly attached to a plant probe with an internal, calibrated light source. The relative reflectance of each leaf was determined from the measurement of leaf radiance divided by the radiance of a 99.9% reflective white standard (Spectralon, Labsphere Inc., North Dutton, NH, USA). Reflectance was measured on ten different areas of each leaf lamina, and the resulting ten spectra were averaged to determine mean optical properties for each leaf. Each measurement required less than 5 s. Measures of leaf optical properties and gas exchange occurred within 24 h of one another.

Leaf nitrogen and leaf mass per area

Immediately following gas exchange and optical assessments, leaves were harvested and measured for projected area using a LI-3100 leaf area meter (Li-Cor Biosciences, Lincoln, NE, USA), oven-dried to a constant mass at 70 °C, and weighed. These data were combined to calculate leaf mass per area (M_{area}, g m^{-2}). Dried leaves were then finely ground and analysed for nitrogen concentration using an Elementar Vario Macro CHN analyser (Elementar Analysensyteme GmbH, Hanau, Germany).

Estimation of leaf photosynthetic traits

Relationships between photosynthesis (A) and intercellular pCO_2 (C_i) were used to estimate maximum rates of RuBP carboxylation (V_{cmax}) and regeneration (J_{max}) at a given leaf temperature with a curve-fitting method that minimized the sums of squares for error resulting from comparisons of observed versus estimated A (Long and Bernacchi, 2003). Michaelis–Menten constants for CO_2 (K_c) and oxygen (K_o), and photosynthetic (CO_2) compensation point (Γ*) were calculated with formulae from Long and Bernacchi (2003). V_{cmax} was estimated from the lower portion of the A–C_i curve (where C_i <30 Pa), and J_{max} was estimated from the upper portion of the curve (C_i >60 Pa). It was noted that this approach does not account for the influence of mesophyll conductance on estimates of V_{cmax} and J_{max} (Dillaway and Kruger, 2010), and thus our reported values are based on intercellular as opposed to chloroplastic pCO_2.

It was assumed that leaf temperature closely tracked air temperature in the glasshouses, and thus, because the two differed somewhat during gas exchange measurements, temperature-response models were used to estimate V_{cmax} and J_{max} for each leaf at its respective glasshouse daytime temperature (i.e. 20, 25, or 30 °C). Temperature-response models were generated for each species based on V_{cmax} and J_{max} data pooled across the three temperature treatments (data not shown). Owing to its exponential form, the temperature sensitivity of V_{cmax} was modelled using an Arrhenius equation (Hikosaka *et al.*, 2006), whereas the asymptotic temperature response of J_{max} was characterized with a 'peak' model (Kattge and Knorr, 2007). The resulting models produced unbiased estimates of V_{cmax} and J_{max} in the cases of both species and all measurement treatments. Specifically, the slopes and intercepts of relationships between observed and predicted V_{cmax} and J_{max} did not differ significantly from 1 and 0, respectively (data not shown). Implicit in this approach was the assumption that photosynthetic metabolism of glasshouse tree foliage did not, to any appreciable extent, acclimate to the different thermal regimes, which would be consistent with our observations in the field (Dillaway and Kruger, 2010).

Generation of predictive models from leaf reflectance spectra

Predictive models of metabolic, biochemical, and morphological traits based on leaf optical properties were examined using partial least-squares regression (PLSR) analysis (Wold *et al.*, 1984; Geladi and Kowalski, 1986; Wolter *et al.*, 2008). While PLSR has not been widely embraced in ecology (Carrascal *et al.*, 2009), its use in remote sensing research has increased in recent years (Smith *et al.*, 2002; Townsend *et al.*, 2003; Ollinger and Smith, 2005; Martin *et al.*, 2008; Wolter *et al.*, 2008). This is because PLSR is useful in situations of high predictor collinearity and/or the predictor variables are equal to or higher than the number of observations, which is often the case in spectroscopic and/or remote sensing research. In addition, models developed using PLSR are much more robust than classical regression in that the calibrated model parameters do not vary greatly given different calibration subsets from a population of observations (i.e. high parameter stability; Geladi and Kowalski, 1986).

A standard PLSR approach for spectral-chemical analysis utilizes the continuous, full-spectrum data (Asner and Martin, 2008; Doughty *et al.*, 2011) or a pre-determined spectral subset (Bolster *et al.*, 1996; Richardson and Reeves, 2005). The spectral loadings (or regression coefficients), which directly relate the target leaf attributes to corresponding spectral features, are generated through the development of a smaller set of orthogonal linear latent components which are obtained through the decomposition of the model variables and the optimization of the covariance structure in the data (Wold *et al.*, 1984; Geladi and Kowalski, 1986; Wolter *et al.*, 2008). In this study, the choice was made to incorporate an automatic variable selection method similar to

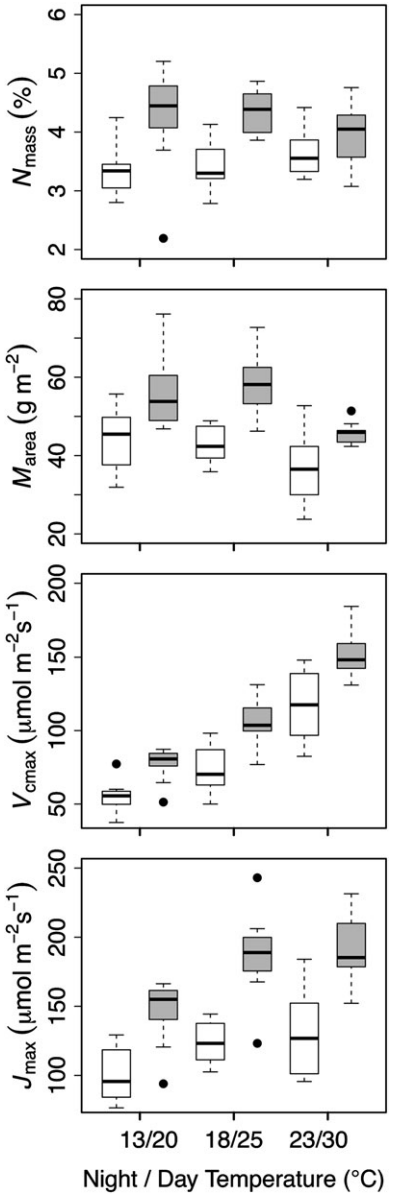

Fig. 1. Variation in nutritional, morphological, and metabolic leaf traits for trembling aspen (white boxes) and eastern cottonwood (grey boxes) measured in the Biotron facility, summarized by night-time/daytime glasshouse temperatures. Traits are nitrogen concentration (N_{mass}, %), leaf mass per area (M_{area}, g m^{-2}), and maximum rates of RuBP carboxylation (V_{cmax}, µmol m^{-2} s^{-1}) and regeneration (J_{max}, µmol m^{-2} s^{-1}). The box plots display the median for each trait by group (dark horizontal line), the interquartile range (IRQ, boxes), the range (whiskers), and the extreme observations (black dots).

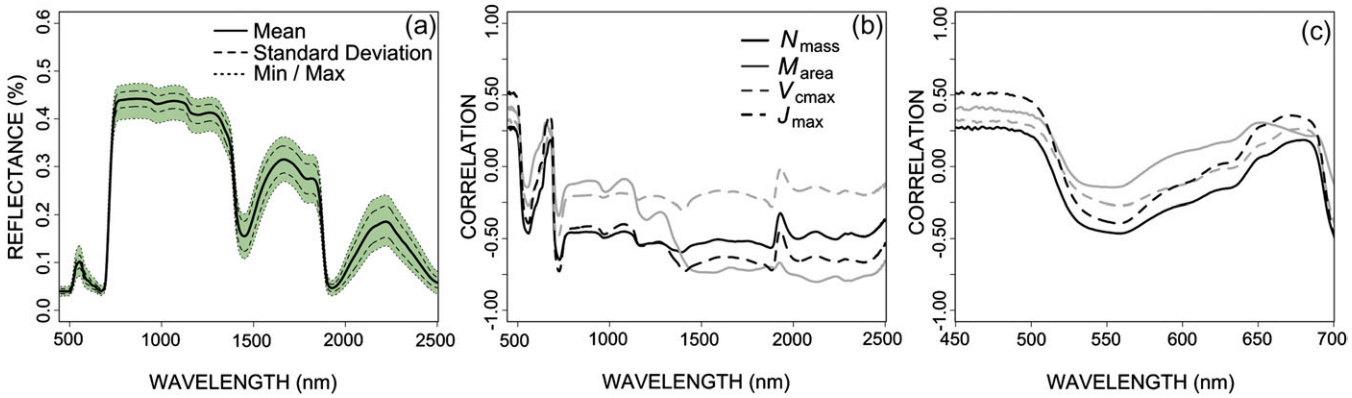

Fig. 2. (a) Mean, ±1 standard deviation, and minimum and maximum leaf reflectance for the pooled aspen and cottonwood seedlings grown in the Biotron facility. Correlation coefficients showing the strength of relationships between spectral wavelengths and each of the four target leaf traits across the full spectrum (b) and for only the visible spectrum (c) Traits are nitrogen concentration (N_{mass}, %), leaf mass per area (M_{area}, g m^{-2}), and maximum rates of RuBP carboxylation (V_{cmax}, μmol m^{-2} s^{-1}) and regeneration (J_{max}, μmol m^{-2} s^{-1}).

Table 1. Summary of two-stage PLSR modelling results for target leaf traits, including nitrogen concentration (N_{mass}, %), leaf mass per area (M_{area}, g m^{-2}), and maximum rates of RuBP carboxylation (V_{cmax}, μmol m^{-2} s^{-1}) and regeneration (J_{max}, μmol m^{-2} s^{-1}).

Variable	Number of wavelengths[a]	Number of components[b]	R^2	RMSE
N_{mass}	13	11	0.89	0.31
M_{area}	11	8	0.95	3.69
V_{cmax}	13	10	0.89	15.4
J_{max}	44	13	0.93	18.67

[a] Number of wavelengths selected in the final PLS models.
[b] Number of PLSR components used to generate the wavelength coefficients in the final models.

Wolter *et al.* (2008) for predictor dimensionality reduction and model optimization. This allowed us to build more parsimonious models and investigate regions of the spectrum that were important for the prediction of each target variable.

The dimensionality reduction involved a two-stage selection of predictor variables (i.e. spectral wavelengths) whereby the variables and number of latent components chosen are those which minimized the model PRESS statistic (Wolter *et al.*, 2008), followed by a second selection technique minimizing the Root Mean Square Error (RMSE), once the model PRESS is minimized. This enabled the continued elimination of redundancy in the spectral data until the model RMSE reached a minimum. In this second step, the iterative-cross validation PRESS statistic (Asner and Martin, 2008; Wolter *et al.*, 2008) was used to select the optimal number of components for each variable subset. The remaining variables and components with the RMSE and PRESS minimized are chosen for the final model. This was done independently for each variable of interest (i.e. V_{cmax}, J_{max}, N_{mass}, and M_{area}). This resulted in PLSR models with only salient variables and components for dependent variable prediction.

The PLSR analysis and variable selection was carried out using the PLSREGRESS function in Matlab (Mathworks, Natick, MA, USA) and a set of custom functions for the variable selection. The entire spectrum from 450–2500 nm was sub-sampled by retaining every fifth wavelength prior to running the analyses to decrease the computation time for variable and component selection. Once the optimal models were chosen, a final PLS-PRESS analysis was carried out to calculate the spectral loadings and model diagnostics.

As additional model verification, a 100× cross-validation of our J_{max} and V_{cmax} models was performed using a random 70/30% split of the data for model calibration and testing. This was done by using the final set of wavelengths and components selected for each variable during the two-stage PLSR modelling to generate new PLSR estimations of the observations left out of each iteration (i.e. 30% validation), based on the remaining data left for calibration (i.e. 70% calibration). The results from this analysis were used to examine model and data stability. From this, the distribution of error resulting from the multiple permutations of the data is reported.

Estimating V_{cmax} and J_{max} with leaf optical data from field-grown aspen

To determine whether the results from our glasshouse PLSR analysis captured short-term (seconds to hours) temperature-dependent variation in leaf metabolic traits rather than–or in addition to–longer-term (days to weeks) photosynthetic acclimation of foliage to variation in growth conditions, leaf properties were examined on five field-grown trembling aspen trees. Measurements were made during an 8 h period on two different days across a range of ambient air temperatures. On 15 July 2009, under clear skies, gas exchange and temperature were measured (on the adaxial and abaxial surface using an Agri-Therm III infrared thermometer, Everest Interscience, Tucson, AZ, USA) on one sunlit leaf per tree in the morning and again in the afternoon. This protocol allowed us to obtain a 5–13 °C span in the temperatures at which a particular leaf was measured.

On a different set of aspen trees, gas exchange and temperature were again measured on one sunlit leaf per tree in the morning and afternoon of 16 June 2010. Here, in addition to measuring leaf temperature just prior to spectral measurements, it was monitored inside the spectroradiometer leaf-clip assembly using a fine-wire thermocouple. This allowed us to test the assumption that spectral measurements did not cause large perturbations of leaf temperature. On average, leaf temperature in the leaf-clip assembly was 0.15 °C (±0.55 °C) higher than the corresponding ambient value.

For these experiments, leaf gas exchange and spectral reflectance were measured in the same fashion as in the glasshouse study, with two exceptions: (i) owing to time constraints, gas exchange measures in July 2009 were confined to the initial portion of the A–C_i curve (cuvette pCO_2 <40 Pa), affording only the estimation of V_{cmax}, while those in June 2010 were confined to cuvette pCO_2

values >60 Pa, affording only the estimation of J_{max}, and (ii) the spectroradiometer was used in its backpack configuration in order to collect leaf spectral data *in situ*. Using these data, the accuracy and precision with which the glasshouse-based PLSR models predicted short-term, temperature-mediated variation in V_{cmax} and J_{max} were examined on an independent set of data under different conditions.

Results

Variation in target leaf traits among glasshouse temperature treatments

In the glasshouses, leaf nitrogen concentration (N_{mass}), leaf mass per area (M_{area}), and maximum rates of RuBP carboxylation (V_{cmax}) and regeneration (J_{max}) varied considerably across temperature regimes and/or species (Fig. 1). Trait responses to growth temperature were fairly consistent across species, except that, as temperature rose, N_{mass} increased in aspen and decreased in cottonwood. N_{mass} and M_{area} were generally higher in cottonwood than in aspen, and for both species M_{area} decreased in the warmest glasshouses. V_{cmax} increased exponentially with temperature, while J_{max} exhibited a less pronounced, asymptotic response. At a given temperature, averages for V_{cmax} and J_{max} were higher in cottonwood than in aspen.

Relationships between target leaf traits and optical properties in the glasshouse

Leaf reflectance varied substantially within and across temperature treatments (Fig. 2a), with a 45%, 20%, and 37% range in reflectance in the visible (450–700 nm), near-infrared (NIR, 700–1300 nm) and shortwave infrared (SWIR, 1500–2500 nm) regions, respectively. The relative range in reflectance for individual wavelengths was at a minimum in the NIR (15% at 772 nm) and peaked in the SWIR (59% at 2494 nm). Target leaf traits were variably correlated (r, 0.25–0.75) with leaf reflectance at wavelengths broadly distributed across the full spectrum (i.e. 450—2500 nm; Fig. 2b). In general, positive correlations were observed in the blue (450–495 nm) and red-edge (650–680 nm) regions, whereas moderate to strong negative correlations occurred in the green (505–570 nm) and red (620–650 nm) regions, and across the NIR and SWIR (Fig. 2b, 2c).

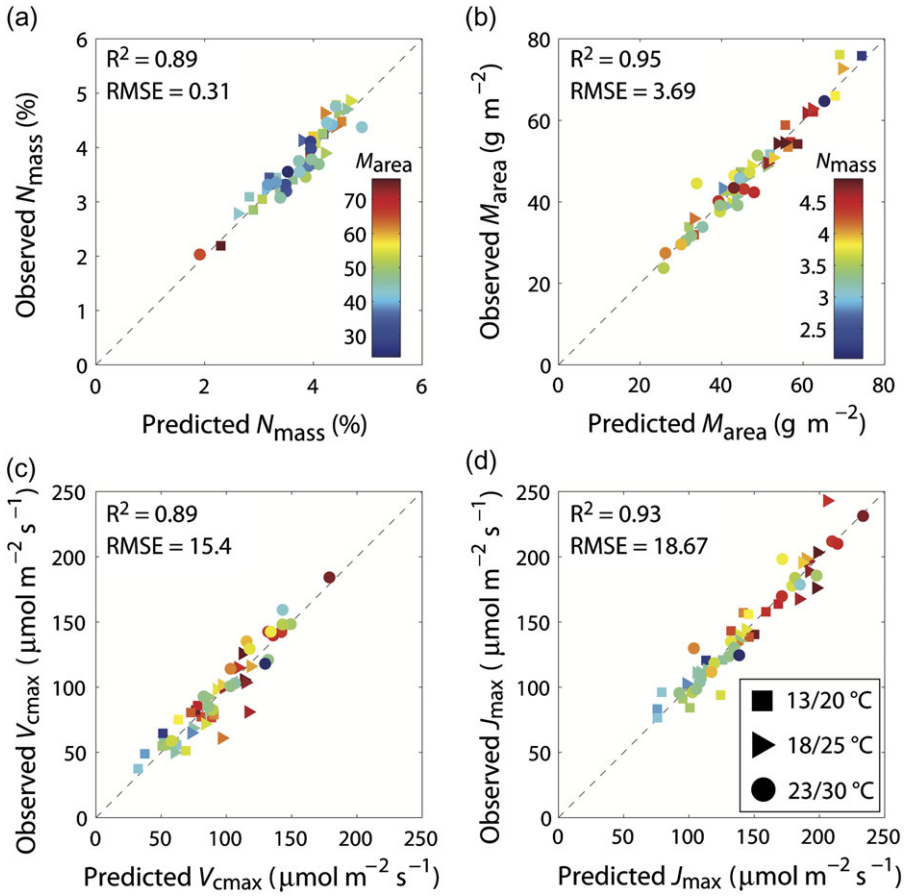

Fig. 3. The observed versus predicted values from the final PLS leave-one-out (LOO) cross-validation procedure for glasshouse leaf nitrogen concentration (N_{mass}, %), leaf mass per area (M_{area}, g m^{-2}), maximum rates of RuBP carboxylation (V_{cmax}, µmol m^{-2} s^{-1}) and regeneration (J_{max}, µmol m^{-2} s^{-1}). Note that the colour scale for N_{mass} (a) depicts corresponding variation in M_{area}, while those for M_{area} (b), V_{cmax} (c), and J_{max} (d) depict variation in N_{mass}. Each plot has a total of 53 observations and the symbols correspond to the three temperate regimes.

PLSR models based on glasshouse data

PLSR analysis yielded accurate and precise empirical predictions of target leaf traits based on leaf reflectance spectra (Table 1; Fig. 3). All models possessed a high coefficient of determination (r^2), while their root mean square error (RMSE) values averaged 8% of the mean. Through automated variable selection, a set of 13 wavelengths was found that described nearly 90% of the variation in V_{cmax} across leaves and temperature treatments, while 44 wavelengths provided an effective model of J_{max} (Table 1). Both the V_{cmax} and J_{max} models involved broadly similar portions within the visible and short-wave spectral regions, although the loadings were generally larger in the V_{cmax} model (Fig. 4; see Supplementary data and Tables S1–S4 at *JXB* online). In contrast to that for V_{cmax}, the model for J_{max} included wavelengths in the NIR related to leaf water content and the green reflectance peak. All models incorporated wavelengths in the visible spectrum (i.e. 450–700 nm), with all but M_{area} including the chlorophyll absorption regions (i.e. ~430–460 nm and 640–670 nm). In addition, wavelength regions included in the J_{max} and V_{cmax} models overlapped somewhat with those selected for the N_{mass} model, while J_{max} further displayed some similarities with M_{area} in the NIR and SWIR (Fig. 4).

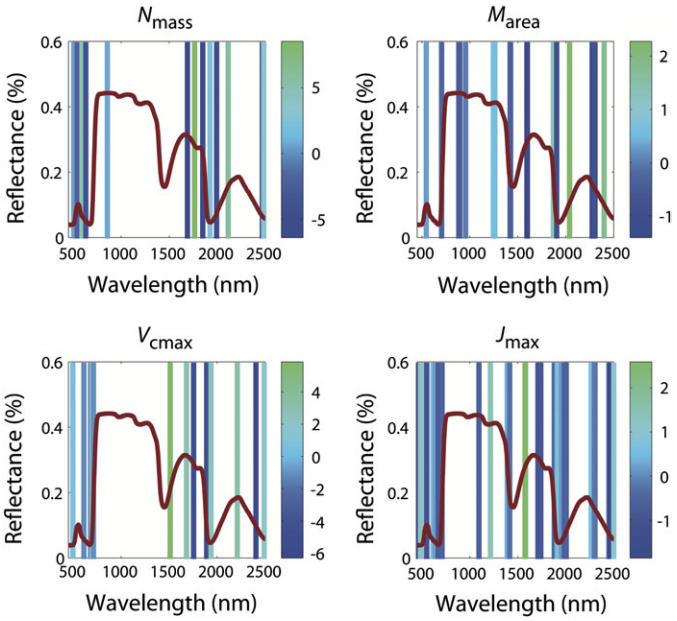

Fig. 4. Final distribution of the wavelengths selected in each two-stage PLSR model for leaf nitrogen concentration (N_{mass}, %), leaf mass per area (M_{area}, g m^{-2}), and maximum rates of RuBP carboxylation (V_{cmax}, μmol m^{-2} s^{-1}) and regeneration (J_{max}, μmol m^{-2} s^{-1}). The colour of each vertical bar represents the magnitude of the standardized variable loading (see colour map). Note that each vertical bar represents only one wavelength and the bar width is exaggerated for display purposes only. The final number of wavelengths selected is 13 for N_{mass}, 11 for M_{area}, 13 for V_{cmax}, and 44 for J_{max} (see Table 1; see Supplementary data and Tables S1–S4 at *JXB* online).

As an additional test of the model stability and robustness for the metabolic parameters (i.e. V_{cmax} and J_{max}), a jackknife test of the glasshouse calibrated PLSR models was performed. The 100× cross-validation analysis showed that the models performed consistently across multiple permutations of the data, with both V_{cmax} (median R^2=0.78, median RMSE=16.2) and J_{max} (median R^2=0.77, median RMSE=20.1) having prediction errors that did not significantly change from the original leave-one-out cross-validation (Fig. 5 shows the R^2 and RMSE histograms for the 100× resampling of the glasshouse models).

Relationships among target leaf traits in the glasshouse

The relationships among target leaf traits, within and across temperature regimes, were examined in an effort to clarify the nature of our PLSR models. In particular, an attempt was made to determine whether predictive models of V_{cmax} and J_{max} might have arisen primarily as a result of the commonly observed dependence of photosynthetic capacity on leaf N status (Field, 1983). To round out this assessment, leaf nitrogen content (N_{area}, the product of M_{area} and N_{mass}) was included in the correlation matrix. Traits were positively correlated with one another in at least one—and often all three—temperature regimes (Fig. 6). In several relationships, however, growth temperature significantly affected the slope and/or intercept. For example, photosynthetic traits were positively correlated with leaf N status (either N_{mass} or N_{area}) within a given temperature regime ($r \geqslant 0.45$, $P \leqslant 0.027$), but, especially in the case of V_{cmax}, the correlations deteriorated when data were pooled across temperatures (Fig. 6). Particularly in relationships among V_{cmax}, J_{max}, and N_{area}, this deterioration resulted from a marked separation of the trend at 30 °C from those at 25 °C and 20 °C (Fig. 4), brought about by the differential temperature responses of each leaf trait (or, in the case of N_{area}, its components N_{mass} and M_{area}) illustrated in Fig. 1.

Predicting the temperature dependence of V_{cmax} and J_{max} in field-grown aspen

In July 2009, averages for leaf temperature and V_{cmax} increased by 7.6 °C (±3.3 °C) and 59.5 μmol m^{-2} s^{-1} (±30.4 μmol m^{-2} s^{-1}), respectively, between morning and afternoon on foliage from the five field-grown aspen trees (Fig. 7a). Using the spectral V_{cmax} model developed with the glasshouse data, it was found that the observed V_{cmax} variation across leaves and temperatures could be predicted with reasonable accuracy and precision (r^2=0.86, RMSE=10.2 μmol m^{-2} s^{-1}) based solely on the corresponding leaf spectral data (Fig. 7c).

In June 2010, on a different set of field-grown aspen, leaf temperature increased by an average of 3.5 °C (±1.3 °C) from morning to afternoon (Fig. 7b), and corresponding J_{max} responses to temperature were variable, showing no clear temperature sensitivity overall. Nevertheless, the spectral J_{max} model yielded precise estimates (r^2=0.93,

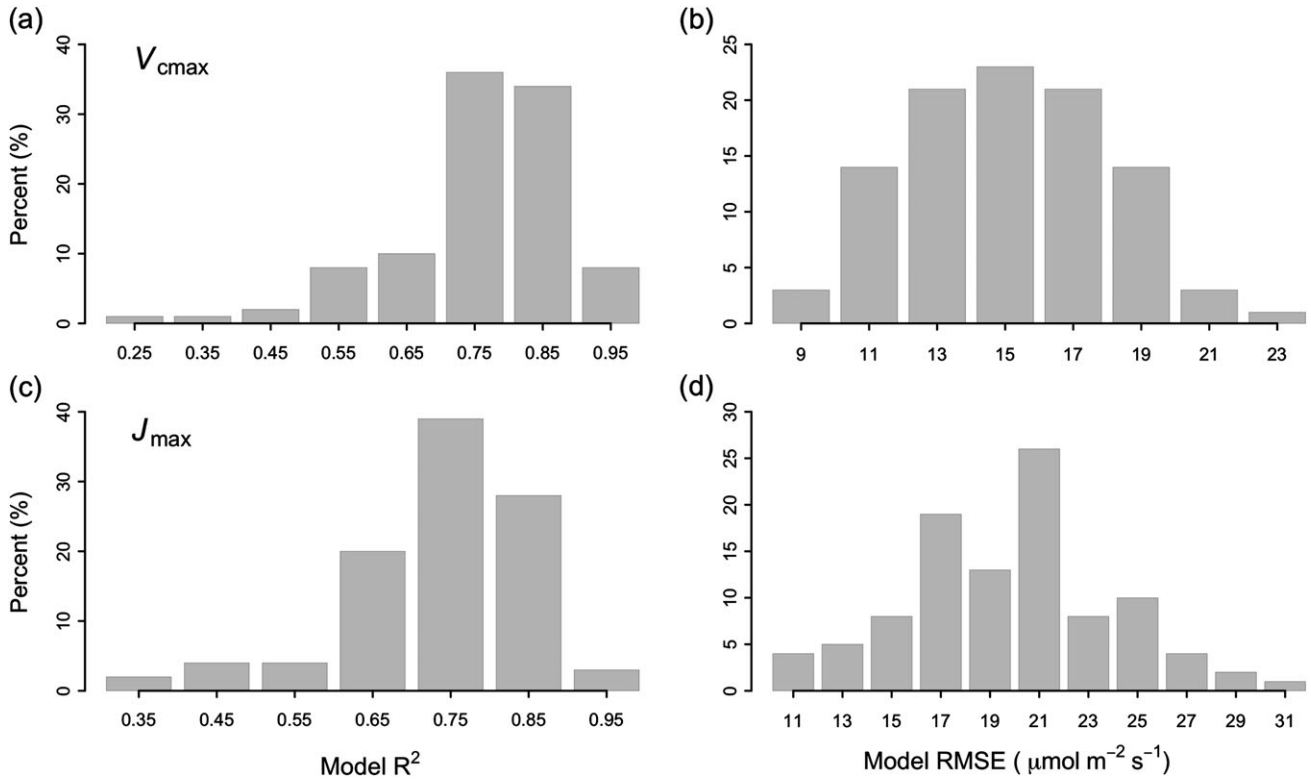

Fig. 5. Results of the 100X jackknife resampling of the PLSR glasshouse models (Fig. 3) for V_{cmax} (a, b) and J_{max} (c, d). The V_{cmax} and J_{max} models had a median R^2 of 0.78 and 0.77, respectively, while the median model RMSE was 16.2 for V_{cmax} and 20.1 for J_{max}.

RMSE=8.2 μmol m^{-2} s^{-1}) based solely the corresponding leaf spectral data (Fig. 7d).

Discussion

Our success in estimating leaf morphology and nitrogen status with spectroscopic models is consistent with previous studies using PLSR approaches (Bolster *et al.*, 1996; Asner and Martin, 2008; Doughty *et al.*, 2011) and other methods (Wessman *et al.*, 1988*a*; McLellan *et al.*, 1991; Kokaly and Clark, 1999). Recently, spectroscopic data combined with PLSR modelling has been used to estimate levels of various other leaf biochemical and nutritional constituents (Gillon *et al.*, 1999; Richardson and Reeves, 2005; Petisco *et al.*, 2006). For example, Asner and Martin (2008) found that spectroscopy could be used to estimate leaf concentrations of chlorophylls (i.e. Chl *a* and Chl *b*), water, carotenoids, and phosphorus. Other studies have provided empirical evidence that concentrations of structural compounds such as lignin and cellulose, as well as tissue ^{13}C and ^{15}N isotopes, can be predicted effectively using the combined spectroscopic PLSR approach (Bolster *et al.*, 1996; Brinkmann *et al.*, 2002; Richardson and Reeves, 2005; Petisco *et al.*, 2006; Kleinebecker *et al.*, 2009).

At present, there is only one other study in the literature (Doughty *et al.*, 2011) that relates the photosynthetic parameters J_{max} and V_{cmax} to full-spectrum leaf optical properties (within a 5 °C temperature range). The authors found weak to moderate predictive power for the V_{cmax} (r^2=0.39, RMSE=36 μmol m^{-2} s^{-1}) and J_{max} models (r^2=0.52, RMSE=39 μmol m^{-2} s^{-1}), in contrast to models of the other variables of interest (e.g. A_{max}, LMA, leaf N). This was attributed to error propagation in the estimation of V_{cmax} and J_{max} (Doughty *et al.*, 2011). On the other hand, Stylinski *et al.* (2000) found a close relationship between J_{max} and the narrow-band photochemical reflectance index (PRI), an optical indicator of the xanthophyll cycle pigments (Gamon *et al.*, 1992; 1997), in foliage of pubescent oak (*Quercus pubescens*) trees. They related this correlation to the down-regulation of electron transport capacity associated with an increase in non-photochemical quenching (NPQ, Demmig-Adams and Adams, 1996, 2006) provided by the xanthophyll cycle pigments.

In addition, Wang *et al.* (2008) observed that an *in situ* broadband simple ratio (SR), based on infrared and photosynthetically active radiation (PAR) reflectance (i.e. 400–700 nm), was a good predictor of the V_{cmax} in Japanese beech (*Fagus crenata*) forests. However, the relationship varied significantly among the three study sites along an elevation gradient, limiting the generality of the results (Wang *et al.*, 2008). As such, a logical continuation of our research effort is an assessment of the utility of our PLSR models across other plant species, regions, and growth environments.

Perhaps the most novel outcome of this study is the apparent ability of spectral reflectance data to capture the short-term temperature sensitivity of V_{cmax} and J_{max}. In particular, our predictive algorithms based on leaf optical

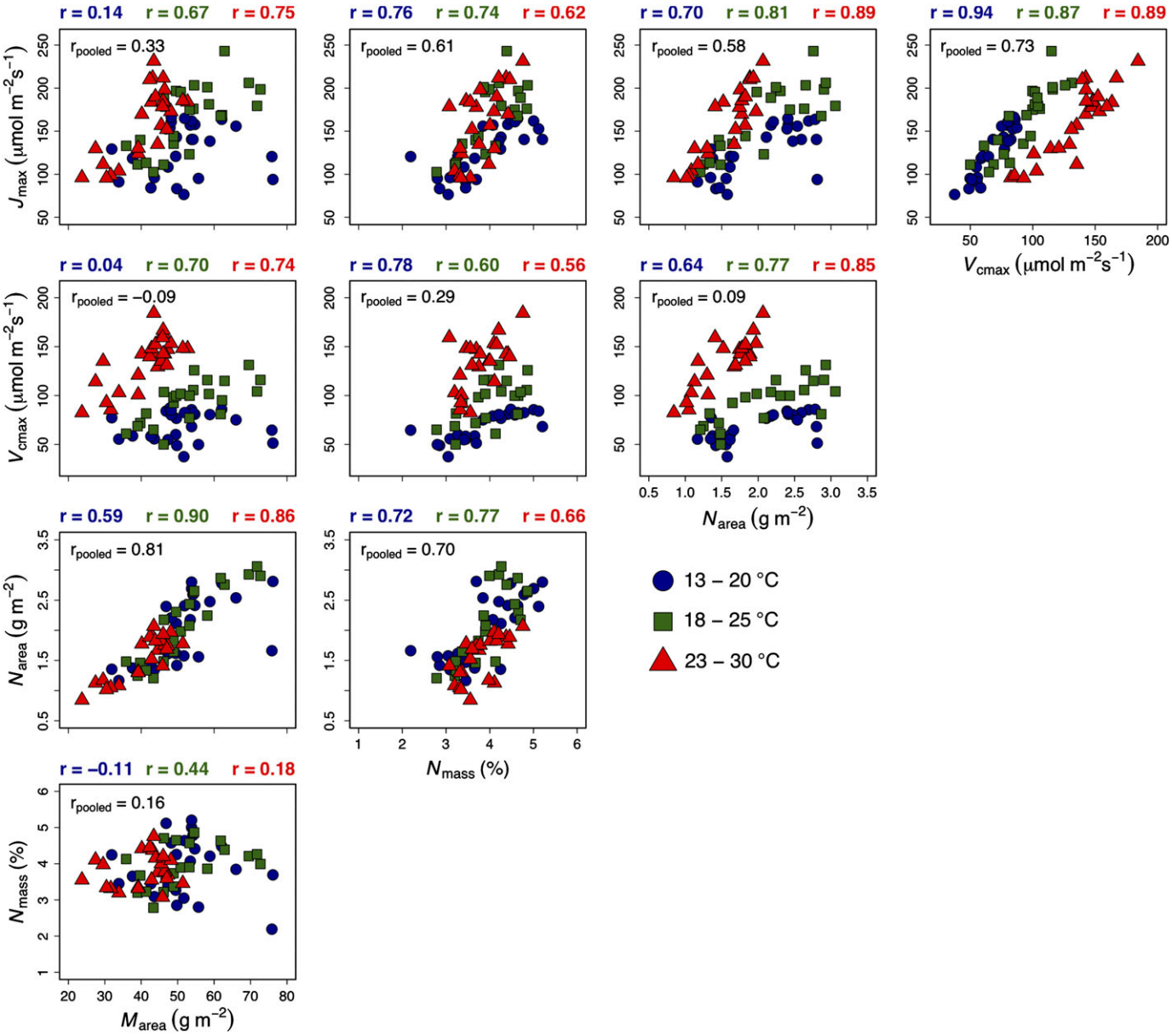

Fig. 6. Relationships among nutritional, morphological, and metabolic leaf traits, including nitrogen concentration (N_{mass}, %), leaf mass per area (M_{area}, g m^{-2}), and maximum rates of RuBP carboxylation (V_{cmax}, μmol m^{-2} s^{-1}) and regeneration (J_{max}, μmol m^{-2} s^{-1}). Note that leaf nitrogen content (N_{area}, g m^{-2}) —the product of M_{area} and N_{mass}—is also included in this analysis. Pearson correlation coefficients (*r*) are presented by temperature treatment and across all data pooled.

properties (Fig. 3) collapsed substantial species- and temperature-mediated variation in V_{cmax} and J_{max} (Fig. 1) into a single trend (Fig. 3c, d). This finding, along with the pronounced temperature-mediated variation observed in certain leaf-trait relationships (Fig. 6), indicate that the derived V_{cmax} and J_{max} PLSR models are not simply scalars of other leaf traits, or of one another. The fact that our glasshouse-based PLSR models for V_{cmax} and J_{max} also performed fairly well when applied to an independent data set of leaves from field-grown trees (Fig. 7c, d) underscores the considerable potential for remote sensing of environmentally sensitive traits governing photosynthetic metabolism in forest canopies.

An examination of the relationship between reflectance and other leaf traits (Fig. 2) highlighted that (i) leaf physiological traits are correlated with leaf optical properties, but the strength of these correlations varies across the VIS/NIR/SWIR regions; and (ii) there are regions of highly collinear wavelengths that allow for reduction of dimensionality in the predictors, potentially without penalty to overall model performance. Although PLSR can handle datasets with high data dimensionality, such as spectral data, appropriate variable selection techniques can enhance the results of PLSR and provide more parsimonious models (Martens and Martens, 2000; Lestander *et al.*, 2003; Schmidtlein *et al.*, 2007; Li *et al.*, 2008; Wolter *et al.*, 2008; Chun and Keles, 2010; Feilhauer *et al.*, 2011).

Use of full-spectrum data can often result in PLSR models with spectral loadings that do not contribute

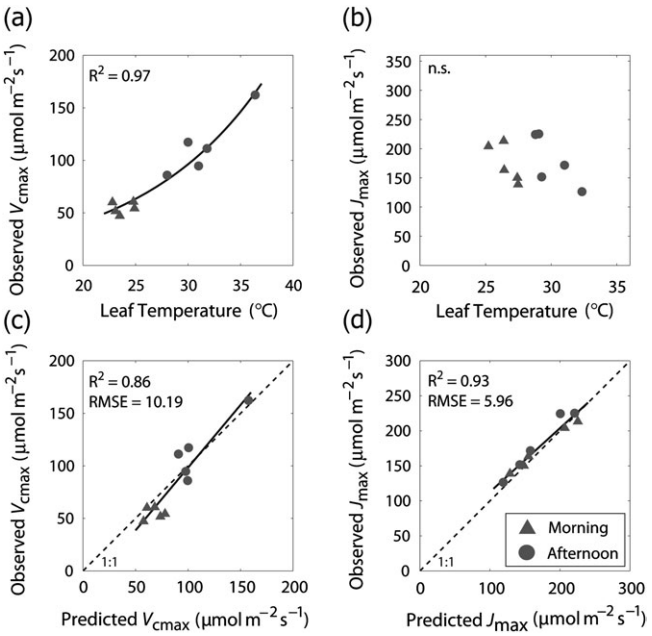

Fig. 7. Relationships between observed V_{cmax} or J_{max} and leaf temperature (a, b), and observed versus PLSR-predicted V_{cmax} or J_{max} (c, d), for field-grown aspen trees. Predicted values are derived using only spectral reflectance data in conjunction with the glasshouse PLSR models (see Supplementary Tables S3 and S4 at *JXB* online), while the observed V_{cmax} and J_{max} data are derived from gas exchange (A–C_i) analyses.

significantly to the prediction (i.e. are near 0) and may negatively affect results (Martens and Martens, 2000; Chun and Keles, 2010). This is important for issues in scaling from the field to broad-scale remote sensing applications where the number of available wavelengths is limited and knowledge of the key spectral regions in predicting the component of interest is important for sensor design. The full-spectrum data was simplified by iteratively removing wavelengths with low predictive power and producing a set of final models with the most significant predictors for each leaf trait (Fig. 4). While there are a variety of PLSR variable selection techniques including genetic algorithm PLS (GA-PLS; Leardi, 2000), interval PLS (iPLS; Norgaard, *et al.*, 2000), sparse PLS (SPLS; Chun and Keles, 2010), and backward selection techniques based on coefficient stability (Martens and Martens, 2000; Feilhauer *et al.*, 2011) the method presented here significantly reduced the spectrum (Table 2; Fig. 4) and provided consistent results for each variable (Fig. 3).

Reviewing the location of selected wavelegnths in our PLSR models (Fig. 4), it was found that many fell within spectral regions associated with leaf characteristics such as internal structure, water content, and chlorophylls. For example, the NIR spectrum of a leaf varies in concert with leaf water content and structure (e.g. thickness and or density), which are related to M_{area} (Jacquemoud and Baret, 1990; Fourty and Baret, 1997; Ceccato *et al.*, 2001). Specifically, leaves require more dry material, structurally, in order to hold higher water content. Related to this, there

Table 2. The number of wavebands selected for each variable during the two-stage PLSR modelling within the visible (VIS), near-infrared (NIR), short-wave 1 (SWIR1), and short-wave 2 (SWIR2) spectral regions

Variable	VIS 400–700 nm	NIR 700–1300 nm	SWIR1 1300–1900 nm	SWIR2 1900–2500 nm
N_{mass}	4	1	3	5
M_{area}	2	8	6	7
V_{cmax}	4	1	4	4
J_{max}	7	3	14	20

are two well-known water absorption features centred at around 970 nm and 1200 nm (Elvidge, 1990; Penuelas *et al.*, 1993; Sims and Gamon, 2003; Kokaly *et al.*, 2009), where both the J_{max} and M_{area} models contain selected wavelengths (Fig. 4). With the exception of the model for M_{area}, all PLSR models contained wavelengths with relatively high spectral loadings in regions with known sensitivities to variations in leaf nitrogen, which occurs primarily in mesophyll proteins and chlorophylls. Nitrogen typically comprises 6.5% (by weight) of the primary light-harvesting molecules and 30–50% of green leaf N is allocated to the protein ribulose-1,5 *bis*phosphate carboxylase-oxygenase (Rubisco; Elvidge, 1990). In total, roughly 70% of leaf N is invested in compounds that support carbon fixation (Field, 1983; Evans, 1989) and leaf N status is often strongly associated with net photosynthetic capacity (A_{max}; Field and Mooney, 1986; Evans, 1989; Reich *et al.*, 1997). Notably, Rubisco has several relatively broad spectral absorption features in the NIR and SWIR centred at 1.5, 1.68, 1.74, 1.94, 2.05, 2.17, 2.29, and 2.47 μm (Elvidge, 1990) that are located in close proximity to several of the wavelength regions selected for leaf N_{mass}, V_{cmax}, and J_{max} (Fig. 4). For example, the V_{cmax} model had wavelengths selected at 1.51, 1.68, 1.76, 1.94, 2.21, and 2.49 μm (Fig. 4: see Supplementary data and Tables S1–S4 at *JXB* online). These considerations further highlight and reinforce plausible linkages between leaf photosynthetic metabolism and spectral reflectance data.

Remote-sensing approaches offer the potential to estimate the landscape- to regional-scale carbon, water, and energy fluxes, as well as other aspects of terrestrial ecosystem function (Carter, 1998; Rahman *et al.*, 2001; Townsend *et al.*, 2003; Fuentes *et al.*, 2006; Asner and Martin, 2008; Hashimoto *et al.*, 2008). As a consequence, there has been much research focused on the development of methods to relate remotely sensed observations, from the shortwave (i.e. 0.3–3 μm) through the mid-infrared and thermal (i.e. 8–15 μm) wavelengths, to the photosynthetic functioning of vegetation (Sellers *et al.*, 1992; Gamon *et al.*, 1997; Carter, 1998; Zarco-Tejada *et al.*, 2003; Grace *et al.*, 2007; Anderson *et al.*, 2008; Hilker *et al.*, 2008; Sims *et al.*, 2008). The spectroscopic technique presented in this study complements previous remote sensing methods that utilize vegetation indices (Gamon *et al.*, 1997; Fuentes *et al.*, 2006; Sims *et al.*, 2008), fluorescence observations (Louis *et al.*,

2005; Damm *et al.*, 2010; Joiner *et al.*, 2011) or light-use efficiency (LUE; Monteith, 1972, 1977) approaches (Rahman *et al.*, 2001; Asner *et al.*, 2004; Hilker *et al.*, 2008) to estimate vegetation carbon fluxes. In this study, hyperspectral data were used to empirically estimate parameters that provide a mechanistic link to the biochemistry of carbon assimilation (Farquhar *et al.*, 1980; Sellers *et al.*, 1992). The method described here can potentially provide rapid and accurate assessments of key metabolic properties at the leaf level. In addition, this approach offers the opportunity to enhance or validate other methods through the integration with long-term monitoring networks such as FLUXNET (Baldocchi *et al.*, 2001) and SpecNet (Gamon *et al.*, 2006). SpecNet, in particular, is designed to explore the linkages between optical remote-sensing data and key parameters governing the exchange of CO_2 and water between vegetation and the atmosphere.

The methods presented here and by others (Doughty *et al.*, 2011) may also provide the basis for regional estimation of photosynthetic metabolism using imaging spectrometers such as the Airborne Visible/Infrared Imaging Spectrometer (AVIRIS; Green *et al.*, 1998) as well as future instruments such as the Hyperspectral Infrared Imager [HyspIRI, a two sensor platform having a spectrometer (400–2500 nm) and an 8-band multi-spectral thermal instrument]. Utilizing such instruments, the potential exists to map parameters such as V_{cmax} and J_{max} while providing empirical and broad-scale observations that can be used to test for photosynthetic thermal acclimation in plants across large climatic gradients (Dillaway and Kruger, 2010; Gunderson *et al.*, 2010). These observations could further be used to improve the parameterization of regional as well as dynamic global vegetation models (DGVMs; Kucharik *et al.*, 2000; Sitch *et al.*, 2003; Krinner *et al.*, 2005; Alton *et al.*, 2007) that rely on the Farquhar–von Caemmerer–Berry model of photosynthesis (Farquhar *et al.*, 1980; Farquhar and Sharkey, 1982).

Supplementary data

Supplementary data can be found at *JXB* online.

Further details of the four PLSR models, including the wavelengths selected and corresponding regression coefficients, are provided. This information can be used to derive estimates of the four traits based on the linear summation of the reflectance values at each wavelength, multiplied by the corresponding regression coefficients, and the intercept value.

Supplementary Table S1. Summary of the leaf nitrogen PLSR model wavelengths, regression coefficients, and jackknife statistics.

Supplementary Table S2. Summary of the leaf mass per area PLSR model wavelengths, regression coefficients, and jackknife statistics.

Supplementary Table S3. Summary of the V_{cmax} PLSR model wavelengths, regression coefficients, and jackknife statistics.

Supplementary Table S4. Summary of the J_{max} PLSR model wavelengths, regression coefficients, and jackknife statistics.

Acknowledgements

This research was supported by grants from the University of Wisconsin-Madison Graduate School as well as a NASA Earth and Space Sciences Fellowship (NNX08AV07H) provided to SPS, a NASA Terrestrial Ecology Grant NNX08AN31G to PAT, and an NSF Dissertation Improvement Grant (#0802729) awarded to DND and ELK. We thank Betsy Middleton and one anonymous reviewer for helpful comments that greatly improved an earlier version of this manuscript.

References

Alton P, Mercado L, North P. 2007. A sensitivity analysis of the land-surface scheme JULES conducted for three forest biomes: biophysical parameters, model processes, and meteorological driving data. *Global Biogeochemical Cycles* **20,** GB1008, doi:10.1029/2005GB002653

Ananyev G, Kolber ZS, Klimov D, Falkowski PG, Berry JA, Rascher U, Martin R, Osmond B. 2005. Remote sensing of heterogeneity in photosynthetic efficiency, electron transport and dissipation of excess light in *Populus deltoides* stands under ambient and elevated CO_2 concentrations, and in a tropical forest canopy, using a new laser-induced fluorescence transient device. *Global Change Biology* **11,** 1195–1206.

Anderson MC, Norman JM, Kustas WP, Houborg R, Starks PJ, Agam N. 2008. A thermal-based remote sensing technique for routine mapping of land-surface carbon, water and energy fluxes from field to regional scales. *Remote Sensing of Environment* **112,** 4227–4241.

Anonymous. 2005. *Using the Li-6400 portable gas exchange system, Version 5*. Lincoln, NE, USA: Li-Cor Biosciences Inc.

Asner GP, Nepstad D, Cardinot G, Ray D. 2004. Drought stress and carbon uptake in an Amazon forest measured with spaceborne imaging spectroscopy. *Proceedings of the National Academy of Sciences, USA* **101,** 6039–6044.

Asner GP, Martin RE. 2008. Spectral and chemical analysis of tropical forests: scaling from leaf to canopy levels. *Remote Sensing of Environment* **112,** 3958–3970.

Asner GP, Martin RE, Tupayachi R, Emerson R, Martinez P, Sinca F, Powell GVN, Wright SJ, Lugo AE. 2011. Taxonomy and remote sensing of leaf mass per area (LMA) in humid tropical forests. *Ecological Applications* **21,** 85–98.

Baldocchi D, Falge E, Gu LH, *et al.* 2001. FLUXNET: a new tool to study the temporal and spatial variability of ecosystem-scale carbon dioxide, water vapor, and energy flux densities. *Bulletin of the American Meteorological Society* **82,** 2415–2434.

Biewer S, Fricke T, Wachendorf M. 2009. Development of canopy reflectance models to predict forage quality of legume–grass mixtures. *Crop Science* **49,** 1917–1926.

Bolster KL, Martin ME, Aber JD. 1996. Determination of carbon fraction and nitrogen concentration in tree foliage by near infrared reflectance: a comparison of statistical methods. *Canadian Journal of Forest Research* **26,** 590–600.

Brinkmann K, Blaschke L, Polle A. 2002. Comparison of different methods for lignin determination as a basis for calibration of near-infrared reflectance spectroscopy and implications of lignoproteins. *Journal of Chemical Ecology* **28,** 2483–2501.

Campbell PKE, Middleton EM, Corp LA, Kim MS. 2008. Contribution of chlorophyll fluorescence to the apparent vegetation reflectance. *Science of the Total Environment* **404,** 433–439.

Carrascal LM, Galván I, Gordo O. 2009. Partial least squares regression as an alternative to current regression methods used in ecology. *Oikos* **118,** 681–690.

Carter GA. 1998. Reflectance wavebands and indices for remote estimation of photosynthesis and stomatal conductance in pine canopies. *Remote Sensing of Environment* **63,** 61–72.

Ceccato P, Flasse S, Tarantola S, Jacquemoud S, Gregoire JM. 2001. Detecting vegetation leaf water content using reflectance in the optical domain. *Remote Sensing of Environment* **77,** 22–33.

Cheng YB, Ustin SL, Riano D, Vanderbilt VC. 2008. Water content estimation from hyperspectral images and MODIS indexes in Southeastern Arizona. *Remote Sensing of Environment* **112,** 363–374.

Chun H, Keles S. 2010. Sparse partial least squares regression for simultaneous dimension reduction and variable selection. *Journal of the Royal Statistical Society Series B, Statistical Methodology* **72,** 3–25.

Coops NC, Hilker T, Hall FG, Nichol CJ, Drolet GG. 2010. Estimation of light-use efficiency of terrestrial ecosystem from space: a status report. *Bioscience* **60,** 788–797.

Damm A, Elbers J, Erler A, *et al*. 2010. Remote sensing of sun-induced fluorescence to improve modeling of diurnal courses of gross primary production (GPP). *Global Change Biology* **16,** 171–186.

Demmig-Adams B, Adams WW. 1996. The role of xanthophyll cycle carotenoids in the protection of photosynthesis. *Trends in Plant Science* **1,** 21–26.

Demmig-Adams B, Adams WW. 2006. Photoprotection in an ecological context: the remarkable complexity of thermal energy dissipation. *New Phytologist* **172,** 11–21.

Dillaway DN, Kruger EL. 2010. Thermal acclimation of photosynthesis: a comparison of boreal and temperate tree species along a latitudinal transect. *Plant, Cell and Environment* **33,** 888–899.

Dobrowski SZ, Pushnik JC, Zarco-Tejada PJ, Ustin SL. 2005. Simple reflectance indices track heat and water stress-induced changes in steady-state chlorophyll fluorescence at the canopy scale. *Remote Sensing of Environment* **97,** 403–414.

Doughty C, Asner G, Martin R. 2011. Predicting tropical plant physiology from leaf and canopy spectroscopy. *Oecologia* **165,** 289–299.

Drolet GG, Middleton EM, Huemmrich KF, Hall FG, Amiro BD, Barr AG, Black TA, McCaughey JH, Margolis HA. 2008. Regional mapping of gross light-use efficiency using MODIS spectral indices. *Remote Sensing of Environment* **112,** 3064–3078.

Elvidge CD. 1990. Visible and near-infrared reflectance characteristics of dry plant materials. *International Journal of Remote Sensing* **11,** 1775–1795.

Evans JR. 1989. Photosynthesis and nitrogen relationships in leaves of C_3 plants. *Oecologia* **78,** 9–19.

Farquhar GD, Sharkey TD. 1982. Stomatal conductance and photosynthesis. *Annual Review of Plant Physiology and Plant Molecular Biology* **33,** 317–345.

Farquhar GD, von Caemmerer S. 1982. Modeling photosynthetic response to environmental conditions. In: Lange OL, Nobel PS, Osmond CB, Ziegler H, eds. *Encyclopedia of plant physiology*, Vol. 12B. Berlin: Springer-Verlag, 549–587.

Farquhar GD, von Caemmerer S, Berry JA. 1980. A biochemical-model of photosynthetic CO_2 assimilation in leaves of C_3 species. *Planta* **149,** 78–90.

Feilhauer H, Faude U, Schmidtlein S. 2011. Combining isomap ordination and imaging spectroscopy to map continuous floristic gradients in a heterogeneous landscape. *Remote Sensing of Environment* (in press).

Field C. 1983. Allocating leaf nitrogen for the maximization of carbon gain: leaf age as a control on the allocation program. *Oecologia* **56,** 341–347.

Field C, Mooney HA. 1986. The photosynthesis–nitrogen relationship in wild plants. In: Givnish T, ed. On the economy of plant form and *function*. Cambridge: Cambridge University Press, 22–55.

Fourty T, Baret F. 1997. Vegetation water and dry matter contents estimated from top-of-the-atmosphere reflectance data: a simulation study. *Remote Sensing of Environment* **61,** 34–45.

Freedman A, Cavender-Bares J, Kebabian PL, Bhaskar R, Scott H, Bazzaz FA. 2002. Remote sensing of solar-excited plant fluorescence as a measure of photosynthetic rate. *Photosynthetica* **40,** 127–132.

Fuentes DA, Gamon JA, Cheng YF, Claudio HC, Qiu HL, Mao ZY, Sims DA, Rahman AF, Oechel W, Luo HY. 2006. Mapping carbon and water vapor fluxes in a chaparral ecosystem using vegetation indices derived from AVIRIS. *Remote Sensing of Environment* **103,** 312–323.

Gamon JA, Penuelas J, Field CB. 1992. A narrow-waveband spectral index that tracks diurnal changes in photosynthetic efficiency. *Remote Sensing of Environment* **41,** 35–44.

Gamon JA, Rahman AF, Dungan JL, Schildhauer M, Huemmrich KF. 2006. Spectral network (SpecNet): what is it and why do we need it? *Remote Sensing of Environment* **103,** 227–235.

Gamon JA, Serrano L, Surfus JS. 1997. The photochemical reflectance index: an optical indicator of photosynthetic radiation use efficiency across species, functional types, and nutrient levels. *Oecologia* **112,** 492–501.

Geladi P, Kowalski BR. 1986. Partial least-squares regression: a tutorial. *Analytica Chimica Acta* **185,** 1–17.

Gillon D, Houssard C, Joffre R. 1999. Using near-infrared reflectance spectroscopy to predict carbon, nitrogen and phosphorus content in heterogeneous plant material. *Oecologia* **118,** 173–182.

Gitelson AA, Gritz Y, Merzlyak MN. 2003. Relationships between leaf chlorophyll content and spectral reflectance and algorithms for

non-destructive chlorophyll assessment in higher plant leaves. *Journal of Plant Physiology* **160,** 271–282.

Grace J, Nichol C, Disney M, Lewis P, Quaife T, Bowyer P. 2007. Can we measure terrestrial photosynthesis from space directly, using spectral reflectance and fluorescence? *Global Change Biology* **13,** 1484–1497.

Gray SB, Dermody O, DeLucia EH. 2010. Spectral reflectance from a soybean canopy exposed to elevated CO_2 and O_3. *Journal of Experimental Botany* **61,** 4413–4422.

Green RO, Eastwood ML, Sarture CM, *et al*. 1998. Imaging spectroscopy and the Airborne Visible Infrared Imaging Spectrometer (AVIRIS. *Remote Sensing of Environment* **65,** 227–248.

Guanter L, Alonso L, Gomez-Chova L, Amoros-Lopez J, Vila J, Moreno J. 2007. Estimation of solar-induced vegetation fluorescence from space measurements. *Geophysical Research Letters* **34,** L08401.

Gunderson CA, O'Hara KH, Campion CM, Walker AV, Edwards NT. 2010. Thermal plasticity of photosynthesis: the role of acclimation in forest responses to a warming climate. *Global Change Biology* **16,** 2272–2286.

Guo JM, Trotter CM. 2004. Estimating photosynthetic light-use efficiency using the photochemical reflectance index: variations among species. *Functional Plant Biology* **31,** 255–265.

Hashimoto H, Dungan JL, White MA, Yang F, Michaelis AR, Running SW, Nemani RR. 2008. Satellite-based estimation of surface vapor pressure deficits using MODIS land surface temperature data. *Remote Sensing of Environment* **112,** 142–155.

Hikosaka K, Ishikawa K, Borjigidai A, Muller O, Onoda Y. 2006. Temperature acclimation of photosynthesis: mechanisms involved in the changes in temperature dependence of photosynthetic rate. *Journal of Experimental Botany* **57,** 291–302.

Hilker T, Coops NC, Hall FG, Black TA, Chen B, Krishnan P, Wulder MA, Sellers PJ, Middleton EM, Huemmrich KF. 2008. A modeling approach for upscaling gross ecosystem production to the landscape scale using remote sensing data. *Journal of Geophysical Research-Biogeosciences* **113,** G03006, doi:10.1029/2007JG000666

Jacquemoud S, Baret F. 1990. PROSPECT: a model of leaf optical properties spectra. *Remote Sensing of Environment* **34,** 75–91.

Joiner J, Yoshida Y, Vasilkov AP, Corp LA, Middleton EM. 2011. First observations of global and seasonal terrestrial chlorophyll fluorescence from space. *Biogeosciences* **8,** 637–651.

Kattge J, Knorr W. 2007. Temperature acclimation in a biochemical model of photosynthesis: a reanalysis of data from 36 species. *Plant, Cell and Environment* **30,** 1176–1190.

Kattge J, Knorr W, Raddatz T, Wirth C. 2009. Quantifying photosynthetic capacity and its relationship to leaf nitrogen content for global-scale terrestrial biosphere models. *Global Change Biology* **15,** 976–991.

Kleinebecker T, Schmidt SR, Fritz C, Smolders AJP, Holzel N. 2009. Prediction of delta ^{13}C and delta ^{15}N in plant tissues with near-infrared reflectance spectroscopy. *New Phytologist* **184,** 732–739.

Kokaly RF, Asner GP, Ollinger SV, Martin ME, Wessman CA. 2009. Characterizing canopy biochemistry from imaging spectroscopy and its application to ecosystem studies. *Remote Sensing of Environment* **113,** S78–S91.

Kokaly RF, Clark RN. 1999. Spectroscopic determination of leaf biochemistry using band-depth analysis of absorption features and stepwise multiple linear regression. *Remote Sensing of Environment* **67,** 267–287.

Krinner G, Viovy N, Nd Noblet-Ducoudre, Ogee J, Polcher J, Friedlingstein P, Ciais P, Sitch S, Prentice IC. 2005. A dynamic global vegetation model for studies of the coupled atmosphere–biosphere system. *Global Biogeochemical Cycles* **19,** GB1015, doi:10.1029/2003GB002199

Kucharik CJ, Foley JA, Delire C, Fisher VA, Coe MT, Lenters JD, Young-Molling C, Ramankutty N, Norman JM, Gower ST. 2000. Testing the performance of a dynamic global ecosystem model: water balance, carbon balance, and vegetation structure. *Global Biogeochemical Cycles* **14,** 795–825.

Leardi R. 2000. Application of genetic algorithm–PLS for feature selection in spectral data sets. *Journal of Chemometrics* **14,** 643–655.

Lestander TA, Leardi R, Geladi P. 2003. Selection of near infrared wavelengths using genetic algorithms for the determination of seed moisture content. *Journal of Near Infrared Spectroscopy* **11,** 433–446.

Li L, Cheng YB, Ustin S, Hu XT, Riaño D. 2008. Retrieval of vegetation equivalent water thickness from reflectance using genetic algorithm (GA)–partial least squares (PLS) regression. *Advances in Space Research* **41,** 1755–1763.

Long SP, Bernacchi CJ. 2003. Gas exchange measurements, what can they tell us about the underlying limitations to photosynthesis? Procedures and sources of error. *Journal of Experimental Botany* **54,** 2393–2401.

Louis J, Ounis A, Ducruet JM, *et al*. 2005. Remote sensing of sunlight-induced chlorophyll fluorescence and reflectance of Scots pine in the boreal forest during spring recovery. *Remote Sensing of Environment* **96,** 37–48.

Martens H, Martens M. 2000. Modified Jack-knife estimation of parameter uncertainty in bilinear modelling by partial least squares regression (PLSR). *Food Quality and Preference* **11,** 5–16.

Martin ME, Aber JD. 1997. High spectral resolution remote sensing of forest canopy lignin, nitrogen, and ecosystem processes. *Ecological Applications* **7,** 431–443.

Martin ME, Plourde LC, Ollinger SV, Smith ML, McNeil BE. 2008. A generalizable method for remote sensing of canopy nitrogen across a wide range of forest ecosystems. *Remote Sensing of Environment* **112,** 3511–3519.

McLellan TM, Aber JD, Martin ME, Melillo JM, Nadelhoffer KJ. 1991. Determination of nitrogen, lignin, and cellulose content of decomposing leaf material by near-infrared reflectance spectroscopy. *Canadian Journal of Forest Research* **21,** 1684–1688.

Medlyn BE, Berbigier P, Clement R, Grelle A, Loustau D, Linder S, Wingate L, Jarvis PG, Sigurdsson BD, McMurtrie RE. 2005. Carbon balance of coniferous forests growing in contrasting climates: model-based analysis. *Agricultural and Forest Meteorology* **131,** 97–124.

Medlyn BE, Dreyer E, Ellsworth D, *et al*. 2002. Temperature response of parameters of a biochemically based model of photosynthesis. II. A review of experimental data. *Plant, Cell and Environment* **25,** 1167–1179.

Middleton EM, Cheng Y, Hilker T, Black TA, Praveena K, Coops NC, Huemmrich KF. 2009. Linking foliage spectral responses to canopy-level ecosystem photosynthetic light-use efficiency at a Douglas-fir forest in Canada. *Canadian Journal of Remote Sensing* **35,** 166–188.

Monteith JL. 1972. Solar-radiation and productivity in tropical ecosystems. *Journal of Applied Ecology* **9,** 747–766.

Monteith JL. 1977. Climate and efficiency of crop production in Britain. *Philosophical Transactions of the Royal Society of London Series B, Biological Sciences* **281,** 277–294.

Moorthy I, Miller JR, Noland TL. 2008. Estimating chlorophyll concentration in conifer needles with hyperspectral data: an assessment at the needle and canopy level. *Remote Sensing of Environment* **112,** 2824–2838.

Nichol CJ, Huemmrich KF, Black TA, Jarvis PG, Walthall CL, Grace J, Hall FG. 2000. Remote sensing of photosynthetic light-use efficiency of boreal forest. *Agricultural and Forest Meteorology* **101,** 131–142.

Norgaard L, Saudland A, Wagner J, Nielsen JP, Munck L, Engelsen SB. 2000. Interval partial least-squares regression (iPLS): acomparative chemometric study with an example from near-infrared spectroscopy. *Applied Spectroscopy* **54,** 413–419.

Ollinger SV, Smith ML. 2005. Net primary production and canopy nitrogen in a temperate forest landscape: An analysis using imaging spectroscopy, modeling and field data. *Ecosystems* **8,** 760–778.

Penuelas J, Filella I, Biel C, Serrano L, Save R. 1993. The reflectance at the 950–970 nm region as an indicator of plant water status. *International Journal of Remote Sensing* **14,** 1887–1905.

Penuelas J, Filella I, Gamon JA. 1995. Assesment of photosynthetic radiation-use efficiency with spectral reflectance. *New Phytologist* **131,** 291–296.

Penuelas J, Filella I, Llusia J, Siscart D, Pinol J. 1998. Comparative field study of spring and summer leaf gas exchange and photobiology of the mediterranean trees *Quercus ilex* and *Phillyrea latifolia*. *Journal of Experimental Botany* **49,** 229–238.

Petisco C, Garcia-Criado B, Mediavilla S, de Aldana BRV, Zabalgogeazcoa I, Garcia-Ciudad A. 2006. Near-infrared reflectance spectroscopy as a fast and non-destructive tool to predict foliar organic constituents of several woody species. *Analytical and Bioanalytical Chemistry* **386,** 1823–1833.

Rahman AF, Gamon JA, Fuentes DA, Roberts DA, Prentiss D. 2001. Modeling spatially distributed ecosystem flux of boreal forest using hyperspectral indices from AVIRIS imagery. *Journal of Geophysical Research-Atmospheres* **106,** 33579–33591.

Reich PB, Walters MB, Ellsworth DS. 1997. From tropics to tundra: gobal convergence in plant functioning. *Proceedings of the National Academy of Sciences, USA* **94,** 13730–13734.

Richardson AD, Duigan SP, Berlyn GP. 2002. An evaluation of noninvasive methods to estimate foliar chlorophyll content. *New Phytologist* **153,** 185–194.

Richardson AD, Reeves JB. 2005. Quantitative reflectance spectroscopy as an alternative to traditional wet lab analysis of foliar chemistry: near-infrared and mid-infrared calibrations compared. *Canadian Journal of Forest Research* **35,** 1122–1130.

Schmidtlein S, Zimmermann P, Schupferling R, Weiss C. 2007. Mapping the floristic continuum: ordination space position estimated from imaging spectroscopy. *Journal of Vegetation Science* **18,** 131–140.

Sellers PJ, Berry JA, Collatz GJ, Field CB, Hall FG. 1992. Canopy reflectance, photosynthesis, and transpiration. III. A reanalysis using improved leaf models and a new canopy integration scheme. *Remote Sensing of Environment* **42,** 187–216.

Sims DA, Gamon JA. 2003. Estimation of vegetation water content and photosynthetic tissue area from spectral reflectance: a comparison of indices based on liquid water and chlorophyll absorption features. *Remote Sensing of Environment* **84,** 526–537.

Sims DA, Rahman AF, Cordova VD, *et al*. 2008. A new model of gross primary productivity for North American ecosystems based solely on the enhanced vegetation index and land surface temperature from MODIS. *Remote Sensing of Environment* **112,** 1633–1646.

Sitch S, Smith B, Prentice IC, *et al*. 2003. Evaluation of ecosystem dynamics, plant geography and terrestrial carbon cycling in the LPJ dynamic global vegetation model. *Global Change Biology* **9,** 161–185.

Smith ML, Ollinger SV, Martin ME, Aber JD, Hallett RA, Goodale CL. 2002. Direct estimation of aboveground forest productivity through hyperspectral remote sensing of canopy nitrogen. *Ecological Applications* **12,** 1286–1302.

Stimson HC, Breshears DD, Ustin SL, Kefauver SC. 2005. Spectral sensing of foliar water conditions in two co-occurring conifer species: *Pinus edulis* and *Juniperus monosperma. Remote Sensing of Environment* **96,** 108–118.

Stylinski CD, Oechel WC, Gamon JA, Tissue DT, Miglietta F, Raschi A. 2000. Effects of lifelong [CO_2] enrichment on carboxylation and light utilization of *Quercus pubescens* Willd. examined with gas exchange, biochemistry and optical techniques. *Plant, Cell and Environment* **23,** 1353–1362.

Suarez L, Zarco-Tejada PJ, Sepulcre-Canto G, Perez-Priego O, Miller JR, Jimenez-Munoz JC, Sobrino J. 2008. Assessing canopy PRI for water stress detection with diurnal airborne imagery. *Remote Sensing of Environment* **112,** 560–575.

Thum T, Aalto T, Laurila T, Aurela M, Kolari P, Hari P. 2007. Parametrization of two photosynthesis models at the canopy scale in a northern boreal Scots pine forest. *Tellus Series B, Chemical and Physical Meteorology* **59,** 874–890.

Townsend PA, Foster JR, Chastain RA, Currie WS. 2003. Application of imaging spectroscopy to mapping canopy nitrogen in the forests of the central Appalachian Mountains using Hyperion and AVIRIS. *IEEE Transactions on Geoscience and Remote Sensing* **41,** 1347–1354.

van der Tol C, Verhoef W, Rosema A. 2009. A model for chlorophyll fluorescence and photosynthesis at leaf scale. *Agricultural and Forest Meteorology* **149,** 96–105.

Wang LX, Okin GS, Wang J, Epstein H, Macko SA. 2007. Predicting leaf and canopy ^{15}N compositions from reflectance spectra. *Geophysical Research Letters* **34,** L02401, doi:10.1029/2006GL028506

Wang Q, Iio A, Kakubari Y. 2008. Broadband simple ratio closely traced seasonal trajectory of canopy photosynthetic capacity.

Geophysical Research Letters **35,** L07401, doi:10.1029/2008GL033619

Wessman CA, Aber JD, Peterson DL, Melillo JM. 1988*a*. Foliar analysis using near-infrared reflectance spectroscopy. *Canadian Journal of Forest Research* **18,** 6–11.

Wessman CA, Aber JD, Peterson DL, Melillo JM. 1988*b*. Remote-sensing of canopy chemistry and nitrogen cycling in temperate forest ecosystems. *Nature* **335,** 154–156.

Wold S, Ruhe A, Wold H, Dunn WJ. 1984. The collinearity problem in linear-regression: the partial least-squares (PLS) approach to generalized inverses. *Siam Journal on Scientific and Statistical Computing* **5,** 735–743.

Wolter PT, Townsend PA, Sturtevant BR, Kingdon CC. 2008. Remote sensing of the distribution and abundance of host species for spruce budworm in Northern Minnesota and Ontario. *Remote Sensing of Environment* **112,** 3971–3982.

Wullschleger SD. 1993. Biochemical limitations to carbon assimilation in C_3 plants: a retrospective analysis of the A/C_i curves from 109 species. *Journal of Experimental Botany* **44,** 907–920.

Zarco-Tejada PJ, Pushnik JC, Dobrowski S, Ustin SL. 2003. Steady-state chlorophyll *a* fluorescence detection from canopy derivative reflectance and double-peak red-edge effects. *Remote Sensing of Environment* **84,** 283–294.